

Sorption Characteristics of CO₂ on Rocks and Minerals in Storing CO₂ Processes

Takashi Fujii¹, Satomi Nakagawa¹, Yoshiyuki Sato², Hiroshi Inomata², Toshiyuki Hashida¹

¹Fracture and Reliability Research Institute, Tohoku University, Sendai, Japan; ²Research Center of Supercritical Fluid technology, Tohoku University, Sendai, Japan.

Email: tfujii@rift.mech.tohoku.ac.jp

Received July 8th, 2010; revised August 18th, 2010; accepted August 31st, 2010.

ABSTRACT

As CO₂ is injected into pore spaces of water-filled reservoir rocks, it displaces much of the pore fluids. In short terms (several to tens of years), the greater part of the injected CO₂ is predicted to stay as free CO₂, i.e. in a CO₂ rich dense phase that may contain some water. This paper investigates the sorption characteristics for rocks (quartzose arenite, greywacke, shale, granite and serpentine) and minerals (quartz and albite) in the CO₂ rich dense phase. The measurements were conducted at 50°C and 100°C, and pressures up to 20 MPa. Our results demonstrated that significant quantities of CO₂ were sorbed with all the samples. Particularly, at 50°C and 100°C, quartzose arenite showed largest sorption capacity among the other samples in higher pressures (>10 MPa). Furthermore, comparison with model prediction based on the pore filling model, which assumed that CO₂ acts as filling pore spaces of the rocks and minerals, suggested the importance of the sorption mechanism in the CO₂ geological storage in addition to the pore-filling mechanism. The present results should be pointed out that the sorption characteristics may have significant and meaningful effect on the assessment of CO₂ storage capacity in geological media.

Keywords: Sorption Characteristics, Rocks, Minerals, Storing CO₂ Processes, CO₂ Geological Storage

1. Introduction

It is a well-established fact that the concentrations of CO₂ in the atmosphere have been increasing steadily and has increased globally by about 100 ppm (36%) over the last 250 years, from a range of 275 to 285 ppm in the pre-industrial era to 379 ppm in 2005 [1], and predictions are that, if continuing in a business-as-usual scenario, by the end of this century, humankind will be facing significant climate change, which may affect human health [2]. Thus, a major challenge in mitigating the climate change is a deep reduction of anthropogenic CO₂ emissions to the atmosphere, which hopefully will lead to a stabilization of CO₂ concentration at around 550 ppm (i.e., double of the pre-industrial level). However, the challenge of stabilizing atmospheric CO₂ levels becomes increasingly difficult as the problem matures because fossil fuels, which today provide about 75% of the world's energy, are likely to remain a major component of the world's energy supply for at least the next century.

In recent years, there are a number of ways by which CO₂ emissions can be reduced, among them being CO₂ capture and geological storage (CCGS) technology. CCGS

technology is an enabling technology that will allow the continued use well into this century of fossil fuels for power generation and combustion in industrial processes and also has the potential of the deepest cuts in anthropogenic CO₂ emissions from large stationary sources (e.g., power generation, iron and steel production, cement manufacture). The technology involves the deployment of a set of technologies for capturing CO₂ emitted from the large stationary sources, transporting it usually by pipeline and injecting it into geological storage reservoirs, including depleted oil and gas reservoirs, unminable coal seams, and deep saline aquifers, which is filled with water (most commonly formation brine) into pores spaces of reservoir rocks.

In terms of CO₂ migration process in the deep saline aquifers, if CO₂ moves into, or invades a porous medium saturated with formation brine, the latter is displaced from some of the pore space (a process referred to as drainage) [3], and then the injected CO₂ stays in the injection zone for a long time, is dissolved in the formation brine, and becomes trapped by mineralization. The extent of CO₂-water-rock interaction during migration of the

injected CO₂ is the main control on the fate of the CO₂.

Johnson *et al.* [4] has reported that reactive transport modeling of a Sleipner-like storage reservoir, which is the world's first saline-aquifer CO₂ storage site that the fate and transport of injected CO₂ has been successfully monitored by seismic time-lapse surveys, suggested that 15-20% was still dissolved in the formation brine after 20 years. The remainder stayed as an immiscible condition, *i.e.* in a CO₂ rich dense phase that may contain little water. Consequently, the result from this study indicates that, through the CO₂ migration process within the deep saline aquifers, the fate of injected CO₂ would be predicted to be mostly the immiscible condition in the order of short term storage (e.g. several years or ten years).

Many researchers have investigated about mineral trapping processes among CO₂, water, and rock in CO₂-water-rock system [5-9]. However, interactions among CO₂ and rock that simulates the CO₂ rich dense phase have only been conducted by Lin *et al.* [10].

Up to now, gas sorption isotherm experiments in CO₂/rock or CO₂/water/rock systems have been conducted using shale at 45-50°C and pressures up to 20 MPa [11] and sandstone and granite at 33-200°C, and pressures up to 20 MPa [12-14]. Fujii *et al.* [13,14] indicates that at high pressures (> 10MPa), the amount of CO₂ sorbed by granite is comparable to that by sandstone, but the sorption mechanisms and processes for sandstone, shale, and granite has not been elucidated. Therefore, knowledge of CO₂ sorption characteristics for various rocks will be required for the screening and assessment of suitable CO₂ storage sites for sequestration of CO₂ in geological reservoirs. Thus, for this comparison, in addition to the rock samples reported in the previous literatures, we included samples from other types of rocks (e.g., sedimentary rock, volcanic rock, metamorphic rock) in this experiment. Additionally, to better understand the mechanisms related to sorption of CO₂ on rocks, CO₂ sorption measurements for silica and silicate minerals, which are main component of reservoir rocks, were also conducted.

The purpose of this study is to evaluate sorption characteristics of CO₂ for rocks (sedimentary rocks, metamorphic rocks, and volcanic rocks) and minerals (silica and silicate minerals) in the CO₂ rich dense phase at geological-relevant temperatures and pressures.

2. Experimental

2.1. Samples and Preparation

Samples from five different blocks of rocks (quartzose arenite, greywacke, shale, granite, and serpentine) were used in the experiments. Quartzose arenite and grey-

wacke are well known as quartz-rich sandstone and feldspar-rich sandstone, respectively. In this study, Berea sandstone (from Ohio, USA) and Kimachi sandstone (from Shishido-cho, Shimane, Japan) were chosen as the representation of quartzose arenite and greywacke, respectively.

Berea sandstone composition was determined by point counting (500 points) under a polarizing microscope (OLYMPUS, A6400BX). Berea sandstone consisted mainly of quartz (= 90.7 vol. %), and the observation was in agreement with the results of Wang and Nur (1989). Kimachi sandstone consisted mainly of plagioclase (= 89.9 vol. %) [15]. A sample of shale was obtained from Tedori-group, Niigata, Japan. A sample of granite was obtained from Iidate, Fukushima, Japan. The granite consisted mainly of quartz (= 37.1 vol. %), plagioclase (= 34.0 vol. %) and K-feldspar (= 21.8 vol. %) [15]. A sample of serpentine was obtained from Okaya, Nagano, Japan. Examination of the serpentine using X-ray diffraction verified the abundance of chrysotile and lizardite. Additionally, natural single crystals of quartz (from Alto de Cruzes Santander, Colombia) and albite (from Kotaki, Itoigawa, Niigata, Japan) were used in the experiment. These rock and mineral specimens were shown in **Figure 1**.

The American Society for Testing and Materials (ASTM) procedure [16] was used to determine density and porosity of the samples based on the fundamental Archimedes principle. Specific surface areas were determined by low-pressure nitrogen sorption measurements using the Brunauer-Emmett-Teller (BET) method [17]. The nitrogen sorption measurements were performed at 77 K using a Quantachrome NOVA 2000 series automated volumetric instrument. Prior to each analysis, the samples were degassed at 105°C under vacuum. The obtained values were listed in **Table 1**.

Core specimens of Berea sandstone, Kimachi sandstone, and Iidate granite were cored from these blocks with a thin-wall diamond bits and were cut with a diamond saw. All cores were drilled perpendicular to the bedding plane. These core specimens were each about 16 mm in diameter and about 10 mm in length. The specimen of shale was broken into angular fragments approximately 5 to 10 mm in largest dimension. The specimen of serpentine was cut into approximately 10 × 10 mm² in cross-section and 15 mm in length. The specimens of quartz and albite with dimensions of 65 × 20 mm³ and 10 × 10 × 10 mm³, respectively, were prepared from each natural single crystals.

These cut specimens were washed with distilled water and were dried under vacuum in an oven for at least 24 hours at 105°C using a rotary vacuum pump.



Figure 1. Photographs of rock and mineral specimens tested in the experiment. (a) Berea sandstone; (b) Kimachi sandstone; (c) Shale; (d) Serpentine; (e) Granite; (f) Quartz; (g) Albite.

Table 1. Rocks and minerals properties for CO₂ sorption measurement.

Materials	Specific surface area (m ² /g)	Bulk density (g/cm ³)	Porosity (vol. %)
Kimachi sandstone	2.80	2.51	20.0
Berea sandstone	0.84	2.11	19.0
Granite	-	2.62	1.1
Shale	0.65	2.60	3.4
Serpentine	-	2.51	4.9
Quartz	-	2.60	< 0.1
Albite	-	2.60	0.9

2.2. Apparatus and Procedure

The magnetic suspension balance (MSB) from Rubotherm Präzisionsmesstechnik GmbH [18] rated at 350°C and 35 MPa was used to measure the CO₂ sorption capacity of rocks and minerals, as illustrated in **Figure 2**. The MSB consisted of a sorption chamber that was used to expose the sample to CO₂ at elevated temperatures and pressures, and microbalance, which was isolated from the sample and existed at ambient conditions. All of the details for the MSB and its operational procedures have been described in previous literatures by Sato *et al.* [19] and Blasig *et al.* [20]. A schematic of the experimental apparatus was shown in **Figure 3**. The experimental apparatus consisted of a high CO₂ pressure supply system, which was used to pressurize CO₂ up to 20 MPa, a data acquisition system and a MSB system.

In the experiment, the sorption measurements were performed at 50°C and 100°C, and pressures up to 20 MPa.

In a typical experiment, a sample was weighed and placed in a sample basket suspended by a permanent magnet through an electromagnet, as shown in **Figure 2**. After closing the sorption chamber, the sample was degassed by evacuating the sorption chamber at elevated temperatures until the weight measured by the microbalance remained unchanged over time. A heating circulator (Julabo, model F25) was used to control the temperature of the chamber, which was measured with a calibrated platinum resistance thermometer to an accuracy of ± 0.05

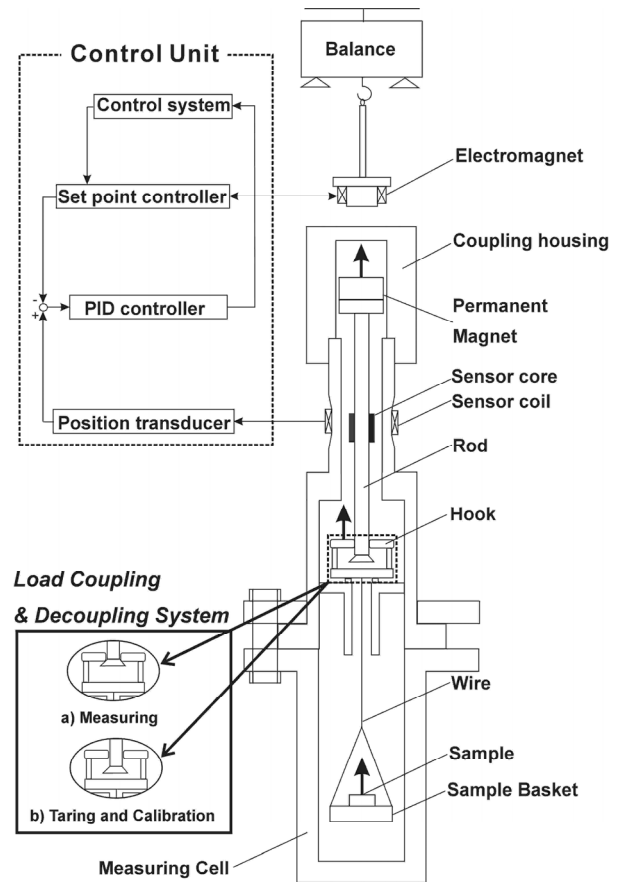


Figure 2. Principle of the magnetic suspension balance (MSB).

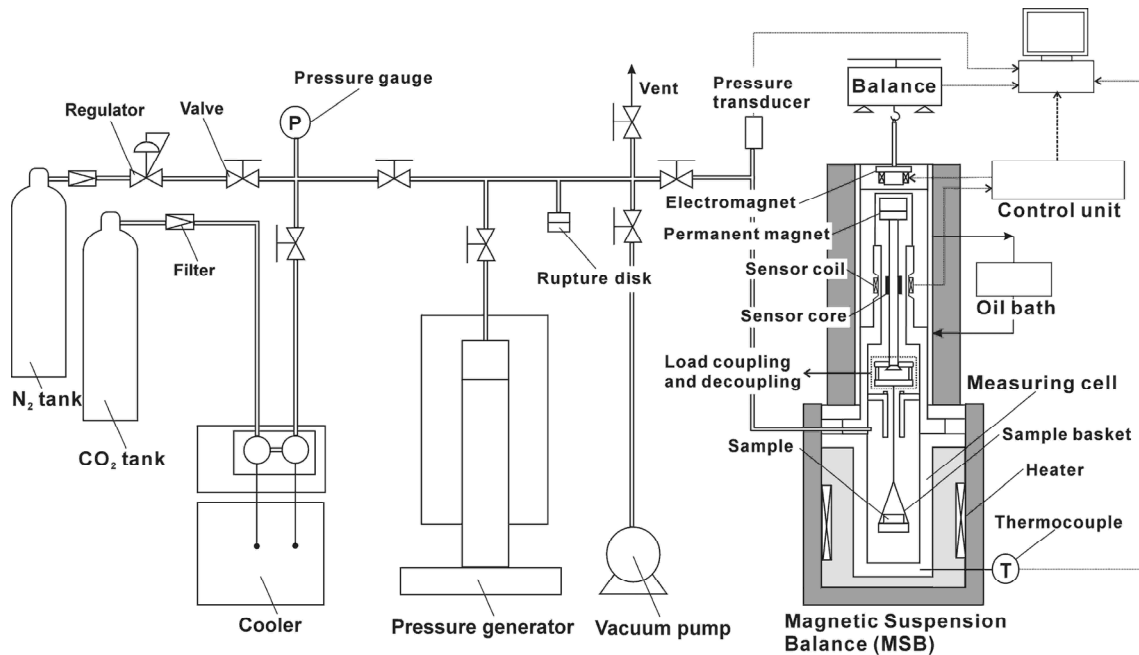


Figure 3. Schematic diagram of the experimental apparatus for CO₂ sorption measurement by using the MSB system (source: Sato *et al.* [19]).

K. The sample weight, read from the microbalance under vacuum and at temperature T , was recorded as $w(vac, T)$ prior to CO₂ injection into the sorption chamber.

CO₂ was introduced into the sorption chamber by the following way. At low pressure up to 5 MPa, the sorption chamber was flooded with CO₂ from a gas cylinder and the pressure was controlled by a regulator. Whereas, at the pressures above 5 MPa, CO₂ was introduced by passing through a high-performance liquid chromatography (HPLC) pump (Jasco 880PU). CO₂ pressure inside the sorption chamber was measured by using Paroscientific pressure transducer (46KR, 41.4 MPa F.S., accuracy 0.01% F.S.).

The change in the mass of the sample as well as the temperature and pressure were measured continuously until the thermodynamic equilibrium was reached. Eventually, an equilibrium sorption was reached, that is, the mass of the sample stopped increasing. The equilibrium sorption was achieved in about 90 minutes at every pressure steps. At this final saturation stage, the weight reading from the microbalance at pressure P and temperature T was recorded as $w(P, T)$.

The mass of the sorbed CO₂ on the rock and mineral samples was calculated based on the consideration of a buoyancy of instruments, which was housed in the sorption chamber, at different gas pressures and different densities as shown in the Equation (1).

Where $n_g^{ex}(P, T)$ was CO₂ sorbed amount on the sample and was termed excess CO₂ sorption capacity. $\rho_{CO_2}(P, T)$ was CO₂ phase density at P and T . m_{CO_2} was the molecular weight. V_r and V_b were the volumes of the sample and of the sample basket, respectively. The last term of the above equation, $\rho_{CO_2}(P, T) \cdot (V_b + V_r)$ represented the buoyancy force caused by the compressed gas, which lifted the sample and sample basket. CO₂ phase density, $\rho_{CO_2}(P, T)$, was calculated from the Wagner EOS [21].

The volume of the sample basket, V_b , was determined using Equation (2) from a buoyancy experiment, that is, the MSB experiment was performed without a sample in the sample basket at the experimental temperature and pressure.

$$V_b = \{w(vac, T) - w(P, T)\} / \rho_{CO_2}(P, T) \quad (2)$$

The result obtained from the buoyancy experiment indicated that, at 50°C and 100°C, the values of the sample basket were constant within limited pressure ranges (~20 MPa) and were 1.69 cm³ at 50 °C and 1.71 cm³ at 100°C, respectively. The volume of the sample, V_r , was calculated from mass and density of the sample.

After the experiment, the samples were reweighed under vacuum condition in the sorption chamber.

3. Results and Discussion

The excess sorption data of CO₂ obtained on the five rock samples (Berea sandstone, Kimachi sandstone, serpentine, shale, granite) and the two mineral samples (quartz and albite) are shown in **Figure 4** under the pressures up to 20 MPa at 50°C in **Figure 4(a)** and 100°C in **Figure 4(b)**, respectively.

The excess sorption data are shown on a sample volume basis in **Figure 4**. It has been shown that shale [11] and sandstone and granite [12-14] have a certain degree of sorption capacities for CO₂ under air-dry conditions. The experimental data obtained in this study confirm the results of the previous literatures. **Figure 4** reveals that the Berea sandstone samples show significantly larger weight changes compared with the other types of rocks, in particular with the Kimachi sandstone samples. The maximum sorption capacity of Berea sandstone for CO₂ exhibits 3.7 mmol/cm³ (= 82.9 cm³ STP/cm³) at 50°C and 20 MPa and 2.8 mmol/cm³ (= 62.7 cm³ STP/cm³) at 100°C and 20 MPa, respectively. It should be mentioned here that the pore volume of Berea sandstone (porosity: ϕ 17.9 vol.%) is slightly smaller than that of Kimachi sandstone (porosity: ϕ 20.0 vol. %). As mentioned in the section of Experimental, B.E.T. tests were carried out to evaluate the specific surface area of the rock samples using N₂ sorption isotherms. Valid experimental data for specific surface area were obtained only for Berea sandstone, Kimachi sandstone, and shale, which showed no dependence of the sample sizes used for the B.E.T. tests. In contrast, the other types of rocks exhibited specific surface areas which varied with the sample size used. In view of the B.E.T. results, the excess sorption data per unit surface area are given only for Berea sandstone, Kimachi sandstone, and shale in **Figures 5(a)** and **5(b)**. It is apparent that Berea sandstone outperforms Kimachi sandstone and shale in the CO₂ sorption capacity.

Coal studies on sorption revealed that maximum excess CO₂ sorption values were approximately 2.0 mmol/g for various coal samples on dry basis at around 50°C [22-24]. Based on CO₂ gravimetric capacity for the rock and mineral samples, at 50°C, maximum CO₂ excess sorption values were approximately 1.8 and 0.5 mmol/g for Berea sandstone and the other rock and mineral samples, respectively. It can, therefore, be said that Berea sandstone exhibits comparable capacity as coals and has a significantly sorption capacity.

$$n_g^{ex}(P, T) = \{w(P, T) - w(vac, T) + \rho_{CO_2}(P, T) \cdot (V_b + V_r)\} / m_{CO_2} \quad (1)$$

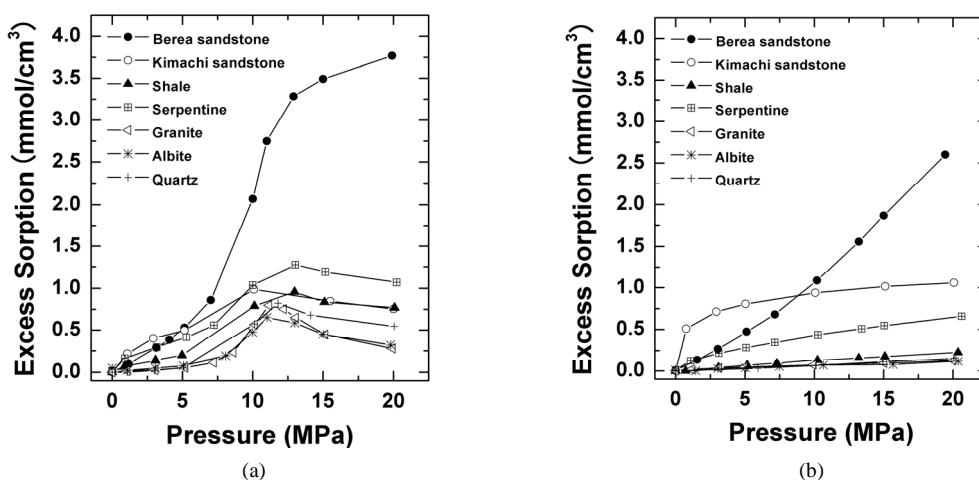


Figure 4. Gravimetric CO₂ excess sorption uptake per unit volume for rocks and minerals under air-dry condition in CO₂/rock or CO₂/mineral systems: (a) at 50°C and (b) at 100°C.

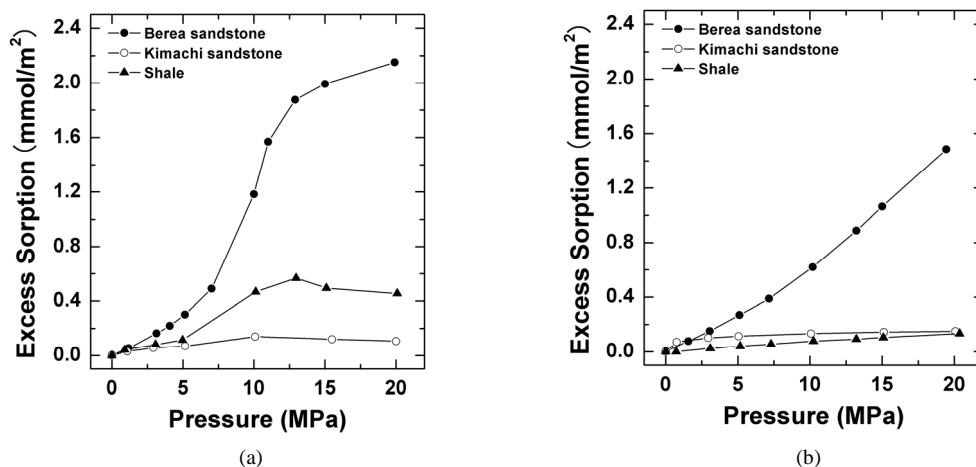


Figure 5. Gravimetric CO₂ excess sorption uptake per unit surface area for rocks and minerals under air-dry condition in CO₂/rock or CO₂/mineral systems: (a) at 50°C and (b) at 100°C.

It is also shown in **Figure 4** that the two mineral samples (quartz and albite) are capable of sorbing CO₂ in the CO₂ rich dense phase. Both quartz and albite is a common and fundamental constituents of most types of rocks. The above result for the quartz and albite samples suggests that the CO₂ sorption capacity of the rocks tested in this study can be attributed to the sorption of CO₂ onto silica and silicate minerals.

It is shown in **Figure 4(a)** that the sorption isotherms at 50°C exhibit a rapid increase in the excess CO₂ sorption for more or less all the rocks and minerals tested, even though the increasing trend is unclear except for Berea sandstone. The rapid increase in the excess CO₂ sorption takes place when the pressure exceeds the critical point of CO₂ (31.0°C, 7.38 MPa) for 50°C. In contrast, the results for 100°C show a nearly linear increase trend with increasing pressure for the majority of the rocks and

minerals. It is interesting to note that the results may correlate with the pressure dependence of CO₂ density. In fact, the CO₂ density shows a sharp jump at the critical point of CO₂ for 50°C, whereas an approximately linear increase is observed for 100°C [21].

The amount of CO₂ sorbed at 50°C decreases with increasing pressure in the higher pressure range (> 10 MPa), except for Berea sandstone. This trend is in agreement with the result reported by Romanov *et al.* [22], who have shown for coal samples that at high pressures above 10 MPa, the amount of CO₂ sorbed reduced as increasing pressure.

The decreasing trend of the sorption isotherms for 50°C in the high pressures may be due to the buoyancy force acting on the volume of sorbed CO₂ phase. The sorbed CO₂ phase may alter the buoyancy of the sample in the ambient CO₂ pressures and temperatures during

the experiment, in addition to the volume of the sample, V_r , the sample basket, V_b , and the other measurement instrument. However, the calculation of the excess CO₂ sorption capacity based on Equation (1) ignores the buoyancy effect of the volume of the sorbed CO₂ phase, thus introducing error. Therefore, the error caused by the above-mentioned buoyancy force would be larger at the high pressure range (above the critical pressure) than the low pressure region (~5 MPa) because the CO₂ density and the sorbed phase volume usually increases as the CO₂ pressure increases. The observation suggests that the buoyancy effect may cause the reduction in the excess sorption for the high pressure range.

The amount of sorbed CO₂ for Berea sandstone, however, showed a monotonous increase with increasing CO₂ pressure, even in the higher pressure range. The comparison suggests that the sorption mechanism may form a denser CO₂ sorbed phase in the case of Berea sandstone. The reason for this is unclear and requires further investigation.

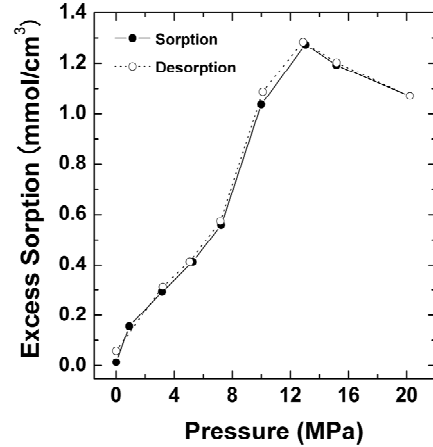
As shown in **Figure 4(b)**, the sorption capacity for 100°C is lower compared with the results for 50°C and shows an approximately linear increase up to 20 MPa, except for Kimachi sandstone.

In contrast, no decreasing trend in the excess sorption is observed for 100°C. Reason for this may be attributed to the decrease of the buoyancy force due to the temperature increase. The buoyancy force associated with sorbed phase volumes was mainly determined by the density of CO₂ phase and CO₂ sorbed phase, and the CO₂ sorption amount. The value of CO₂ density calculated by the Span and Wagner EOS [21] for 100°C and 20 MPa is shown to be approximately half as much as that at 50°C. In addition, the sorbed phase density predicted by Dubinin (1965) [25] decreases with increasing temperature. These results indicate that the buoyancy effect for 100°C is smaller than that for 50°C. Consequently, the error induced by the buoyancy effect for 100°C may be smaller than that for 50°C.

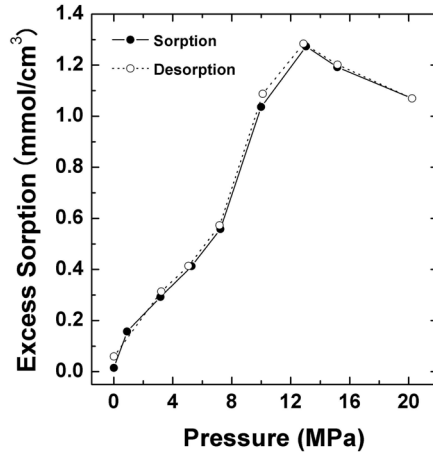
Sorption and desorption isotherms are shown for Berea sandstone and serpentine at 50°C in **Figure 6**. The desorption isotherms coincide approximately with the sorption data. Furthermore, weight measurements for the samples have shown almost no change after the CO₂ sorption experiment. These results indicate the reversible nature of CO₂ sorption-desorption process at 50°C. The same trend has been observed for 100°C.

4. Comparison with Prediction Value Based on Pore-Filling Model

Based on the above discussion, the experimental excess sorption data are corrected for the buoyancy force for the sorbed phase volume using the following equation [26]:



(a)



(b)

Figure 6. Excess sorption and desorption isotherms of CO₂ at 50°C for (a) Berea sandstone and (b) Serpentine under air dry condition in CO₂/rock system.

$$n_g^c = n_g^{ex} \cdot \left(\frac{\rho_a}{\rho_a - \rho_{CO_2}(P, T)} \right) \quad (3)$$

where n_g^c is the CO₂ sorption capacity corrected for the buoyancy effect, n_g^{ex} is the sorbed amount without correction (as measured by the MSB method), $\rho_{CO_2}(P, T)$ is the CO₂ density of the gas phase, and ρ_a is the CO₂ density of the sorbed phase. In this study, we used the sorbed phase density, ρ_a , calculated by Dubinin-Nikolaev formulation [25]. The value of ρ_a is usually assumed to be constant over the entire pressure range at temperatures above the critical temperature (31.1°C). The calculated values of ρ_a at 50 °C and 100 °C were 0.994 g/cm³ and 0.912 g/cm³, respectively. The CO₂ phase density, $\rho_{CO_2}(P, T)$, was calculated from Span and Wagner EOS [21]. The data for the corrected sorption amount are shown in **Figures 7 and 8**. In addition to the corrected CO₂ sorption

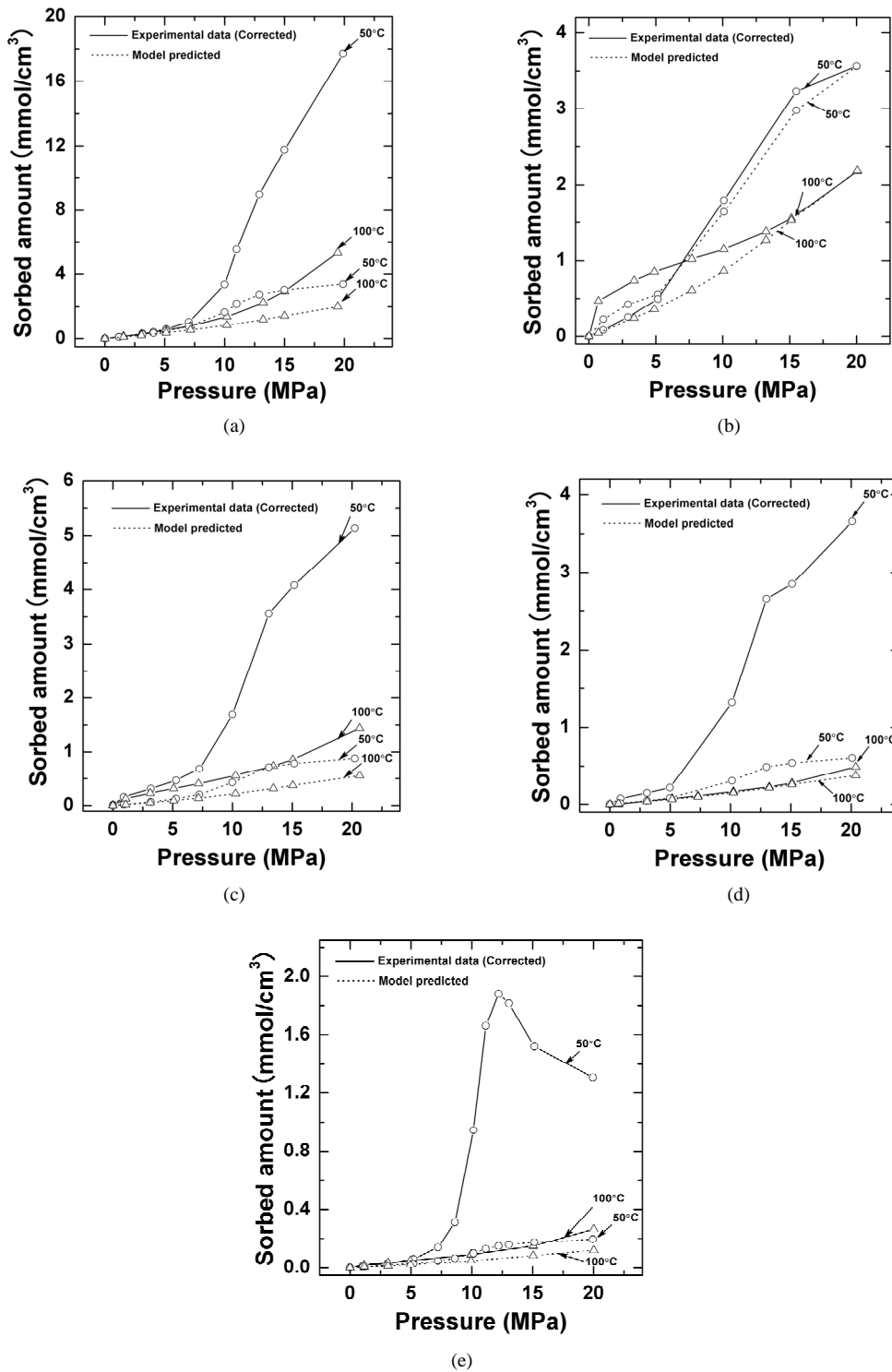


Figure 7. Comparison of the predicted values based on the pore-filling model, with corrected sorption capacity, considering CO₂ sorbed phase density for three sedimentary rocks (Berea sandstone, Kimachi sandstone, and shale), one ultramafic rock (serpentine) and one volcanic rock (granite) at 50°C and 100°C. The solid and dashed lines represent the corrected experimental data and the calculated data, respectively. (ϕ) is the porosity of rock specimens. (a) Berea sandstone (ϕ 19.0); (b) Kimachi sandstone (ϕ 20.0); (c) Serpentine (ϕ 4.9); (d) Shale (ϕ 3.4); (e) Granite (ϕ 1.1).

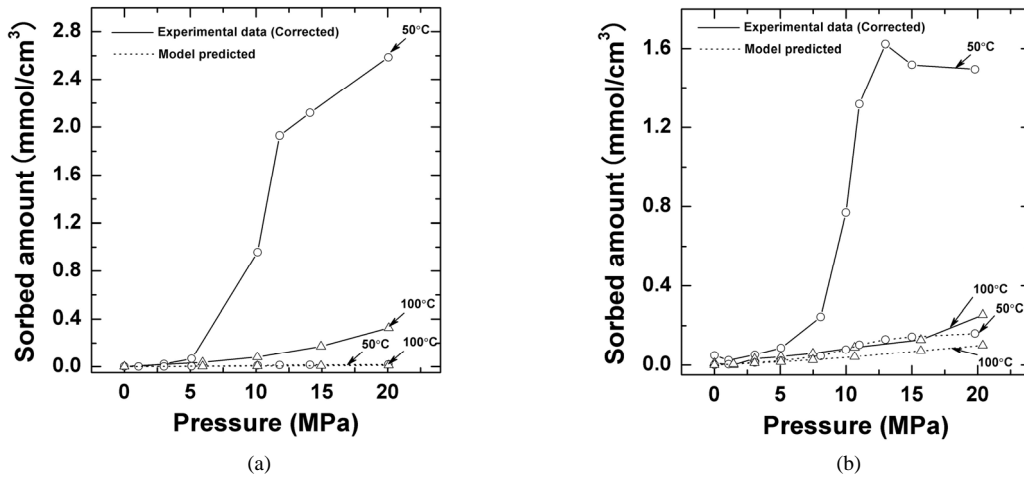


Figure 8. Comparison of the predicted values based on the pore-filling model, with corrected sorption capacity, considering CO₂ sorbed phase density for quartz and albite at 50°C and 100°C. The solid and dashed lines represent the corrected experimental data and the calculated data, respectively. () is the porosity of mineral specimens. (a) Quartz (ϕ 0.1); (b) Albite (ϕ 0.9).

data, the results predicted from the pore-filling model are plotted in these figures. The pore-filling model assumes that the CO₂ storage capacity of the rock mass is equal to the amount of CO₂ used to fill the pore volume in the rock, which is given by the following equation:

$$n_{\text{pore-filling}} = \phi_{\text{rock}} \cdot \rho_{\text{CO}_2} / m_{\text{CO}_2} \quad (4)$$

where ϕ_{rock} is the porosity of the rock sample, and m_{CO_2} is the molecular weight of CO₂. It is seen that the sorption capacity corrected for the buoyancy effect shows a steady increase with respect to pressure at the higher pressure regime, except for the data of the granite and albite at 50°C. The reason for this result probably may be due to the error in estimating the sorbed phase density, and needs to be further investigated in the future. In the lower pressure range (< 5 MPa), the corrected sorption capacity appears to give a value close to that computed based on the pore-filling model. It is demonstrated that the corrected sorption capacity is significantly higher than the model predicted data for the rocks and minerals, except for Kimachi sandstone. For Kimachi sandstone, the corrected result is relatively close to the model predicted data over the entire pressure range. For example, the corrected sorption capacity is shown to be approximately 5 times higher than the model prediction in the case of Berea sandstone, and about 10 times higher for the granite. The comparison may suggest the importance of the sorption mechanism in the CO₂ geological storage in addition to the pore-filling mechanism. The sorption process may provide an additional CO₂ storage mechanism and contribute to the significant part of the CO₂ storage capacity of a rock mass. The effect of water and salinity on the CO₂ sorption capacity is now under inves-

tigation.

5. Conclusions

This paper presents the CO₂ sorption capacities of the five rock samples (Berea sandstone, Kimachi sandstone, shale, serpentine and granite) and the two mineral samples (quartz and albite), measured at 50°C and 100°C, and under pressures up to 20 MPa in CO₂-rock or CO₂-mineral systems that simulate the CO₂ rich dense phase. The CO₂ sorption capacities have been determined by a gravimetric method and corrected for the buoyancy effect. In higher pressure region (> 10 MPa), Berea sandstone has shown a significantly higher CO₂ sorption capacity compared to the other rocks and minerals at both 50°C and 100°C and exhibited a maximum sorption capacity of 3.7 mmol/cm³ (= 82.9 cm³ STP/cm³) at 50°C and 20 MPa and 2.8 mmol/cm³ (= 62.7 cm³ STP/cm³) at 100°C and 20 MPa. Thus, arkosic sandstone such as Berea sandstone may provide a significant potential for CO₂ geological sequestration for a suitable reservoir rock. It is also shown that the major constituent minerals for the rocks tested in this study (quartz and albite) have a CO₂ sorption behavior.

It has been demonstrated that the CO₂ sorption capacity measured in this study is significantly higher than that predicted by the pore-filling model for the rocks and minerals. The comparison suggests that the CO₂ sorption characteristic may provide an important mechanism in the assessment of CO₂ storage capacity in geological media.

REFERENCES

- [1] IPCC, Intergovernmental Panel on Climate Change,

- “Changes in Atmospheric Constituents and in Radiative Forcing (Chapter 2), Fourth Assessment Report of the Working Group I Report,” In: P. Forster, V. Ramaswamy Ed., Cambridge University Press, Cambridge, UK, 2007, p. 137.
- [2] J. Nishizawa and I. Ueno, “The Human Beings Perish from the Earth in Eighty Years,” ToyoKeizaiSinposha, Tokyo, 2000, pp. 7-19.
- [3] S. Bachu, “CO₂ Storage in Geological Media: Role, Means, Status and Barriers to Deployment,” *Progress in Energy and Combustion Science*, Vol. 34, No. 2, 2008, pp. 254-273.
- [4] J. W. Johnson, J. J. Nitao and K. G. Knauss, “Geological Storage of Carbon Dioxide,” In: S. J. Baines and R. H. Worden, Ed., *Geological Society*, Special Publications, London, Vol. 233, 2004, pp. 107-128.
- [5] W. D. Gunter, B. Wiwchar and E. H. Perkins, “Carbon Dioxide Disposal,” Geoscience Publishing Ltd., Alberta, Canada, 1996, pp. 115-122.
- [6] R. Shiraki and T. L. Dunn, “Experimental Study on Water-Rock Interactions during CO₂ Flooding in the Tensleep Formation,” *Applied Geochemistry*, Vol. 15, No. 3, 2000, pp. 265-279.
- [7] C. A. Rochelle, I. Czernichowski-lauriol and A. E. Milodowski, “Geological Storage of Carbon Dioxide,” In: S. J. Baines, & R. H. Worden, Ed., *Geological Society*, Special Publications, London, 2004, pp. 87-106.
- [8] J. P. Kaszuba, D. R. Janecky and M. G. Snow, “Carbon Dioxide Reaction Processes in a Model Brine Aquifer at 200°C and 200 Bars: Implications for Geologic Sequestration of Carbon,” *Applied Geochemistry*, Vol. 18, No.7, 2003, pp. 1065-1080.
- [9] Y. Suto, L. Liu, N. Yamasaki and T. Hashida, “Initial Behavior of Granite in Response to Injection of CO₂-Saturated Fluid,” *Applied Geochemistry*, Vol. 22, No. 1, 2007, pp. 202-218.
- [10] H. Lin, T. Fujii, R. Takisawa, T. Takahashi and T. Hashida, “Experimental Evaluation of Interactions in Supercritical CO₂/Water/Rock Minerals System under Geologic CO₂ Sequestration Conditions,” *Journal of Materials Science*, Vol. 43, No. 7, 2008, pp. 2307-2315.
- [11] A. Busch, S. Alles, Y. Gensterblum, D. Prinz, D. N. Dewhurst, M. D. Raven, H. Stanjek and B. M. Kroose, “Carbon Dioxide Storage Potential of Shales,” *International Journal of Greenhouse Gas Control*, Vol. 2, No. 3, 2008, pp. 297-308.
- [12] T. Fujii, Y. Sato, H. Lin, K. Sasaki, T. Takahashi, H. Inomata and T. Hashida, “Evaluation of CO₂ Sorption Capacity of Granite for CO₂ Geological Sequestration,” *AIP Conference Proceedings*, Vol. 898, 2007, pp. 79-83.
- [13] T. Fujii, Y. Sugai, K. Sasaki and T. Hashida, “Measurements of CO₂ Sorption on Rocks Using a Volumetric Technique for CO₂ Geological Storage,” *Energy Procedia*, Vol. 1, No. 1, 2009, pp. 3715-3722.
- [14] T. Fujii, Y. Sato, H. Lin, H. Inomata and T. Hashida, “Evaluation of CO₂ Sorption Capacity of Rocks Using a Gravimetric Method for CO₂ Geological Sequestration,” *Energy Procedia*, Vol. 1, No. 1, 2009, pp. 3723-3730.
- [15] L. Liu, Y. Suto, G. Bignall, N. Yamasaki and T. Hashida, “CO₂ Injection to Granite and Sandstone in Experimental Rock/Hot Water Systems,” *Energy Conversion & Management*, Vol. 44, No. 9, 2003, pp. 1399-1410.
- [16] ASTM C 20-80a, “Standard Test Methods for Apparent Porosity, Water Absorption, Apparent Specific Gravity, and Bulk Density of Burned Refractory Brick and Shapes by Boiling Water,” *Annual Book of ASTM Standards*, 1981.
- [17] S. Brunauer, P. H. Emmett and E. Teller, “Adsorption of Gases in Multimolecular Layers,” *Journal of the American Chemical Society*, Vol.60, 1938, pp. 309-319.
- [18] R. Kleinrahm and W. Wagner, “Measurement and Correlation of the Equilibrium Liquid and Vapour Densities and the Vapour Pressure along the Coexistence Curve of Methane,” *Journal of Chemical Thermodynamics*, Vol. 18, No. 8, 1986, pp. 739-760.
- [19] Y. Sato, T. Takikawa, S. Takishima and H. Masuoka, “Solubilities and Diffusion Coefficients of Carbon Dioxide in Poly(Vinyl Acetate) and Polystyrene,” *Journal of Supercritical Fluids*, Vol. 18, 2001, pp. 187-198.
- [20] A. Blasig, J. Tang, X. Hu, Y. Shen and M. Radosz, “Magnetic Suspension Balance Study of Carbon Dioxide Solubility in Ammonium-Based Polymerized Ionic Liquids: Poly (P-Vinylbenzyltrimethyl Ammonium Tetrafluoroborate) and Poly ([2-(Methacryloyloxy) Ethyl] Ammonium Tetrafluoroborate),” *Fluid Phase Equilibria*, Vol. 256, 2007, pp. 75-80.
- [21] R. Span and W. Wagner, “A New Equation Of State for Carbon Dioxide Covering the Fluid Region from the Triple-Point Temperature to 1100 K At Pressures up to 800 Mpa,” *Journal of Physical and Chemical Reference Data*, Vol. 25, No. 6, 1996, pp. 1509-1596.
- [22] V. N. Romanov, A. L. Goodman and J. W. Larsen, “Errors in CO₂ Adsorption Measurements Caused by Coal Swelling,” *Energy & Fuels*, Vol. 20, 2006, pp. 415-416.
- [23] N. Siemons and A. Busch, “Measurement and Interpretation of Supercritical CO₂ Sorption on Various Coals,” *International Journal of Coal Geology*, Vol. 69, No. 4, 2007, pp. 229-242.
- [24] D. Li, Q. Liu, P. Weniger, Y. Gensterblum, A. Busch and B. M. Krooss, “High-Pressure Sorption Isotherms and Sorption Kinetics of CH₄ and CO₂ on Coals,” *Fuel*, Vol. 89, No. 3, 2010, pp. 569-580.
- [25] M. M. Dubinin, “Modern State of the Theory of the Volume Filling of Micropore Adsorbents during Adsorption of Gases and Steams on Carbon Adsorbents,” *Zhurnal Fizicheskoi Khimii*, Vol. 39, 1965, pp. 1305-1317.
- [26] P. Dutta, S. Harpalani and B. Prusty, “Modeling of CO₂ Sorption on Coal,” *Fuel*, Vol. 87, No. 10-11, 2008, pp. 2023-2036.